Electronic Supplementary Material (ESI) for New Journal of Chemistry.

Supporting Information for

Nickel-Antimony Nanoparticles Confined in SBA-15 as a Highly Efficient Catalyst for the Hydrogenation of Nitroarenes

Vijaykumar S. Marakatti, Sebastian C. Peter*

New Chemistry Unit, Jawaharlal Nehru Centre for Advanced Scientific
Research, Jakkur, Bangalore-560064, India.

(*Corresponding author: sebastiancp@jncasr.ac.in. Phone: 080-22082998, Fax: 080-22082627))

Main properties of aminopropyl-functionalized SBA-15

The anchoring of nanoparticles on the solid supports such as SBA-15 is carried out by using organic molecules grafted on the solid surface, whose terminal functional groups are selected for their electrostatic or chemical interactions with the nanoparticles. The molecules commonly used for the functionalization are organosilane with up to three hydrolysable groups (either −OR or −Cl) that would react with the silanols groups of the SBA-15 surface and a nonhydrolysable group bearing the terminal function responsible for the interaction with the nanoparticles. Among the large variety of organosilanes, aminopropyltriethoxysilane (APTES) is the most studied surface modifier. APTES is relatively easy to handle due to its moderate reactivity. The three hydrolysable ethoxy groups ensure a robust anchoring of the silane to the surface of support, whereas the amine function of the aminopropyl group remains available for further reaction. Terminal amine functions are extensively used for surface functionalization because they easily react electrostatically with metal ions or metal nanoparticles.

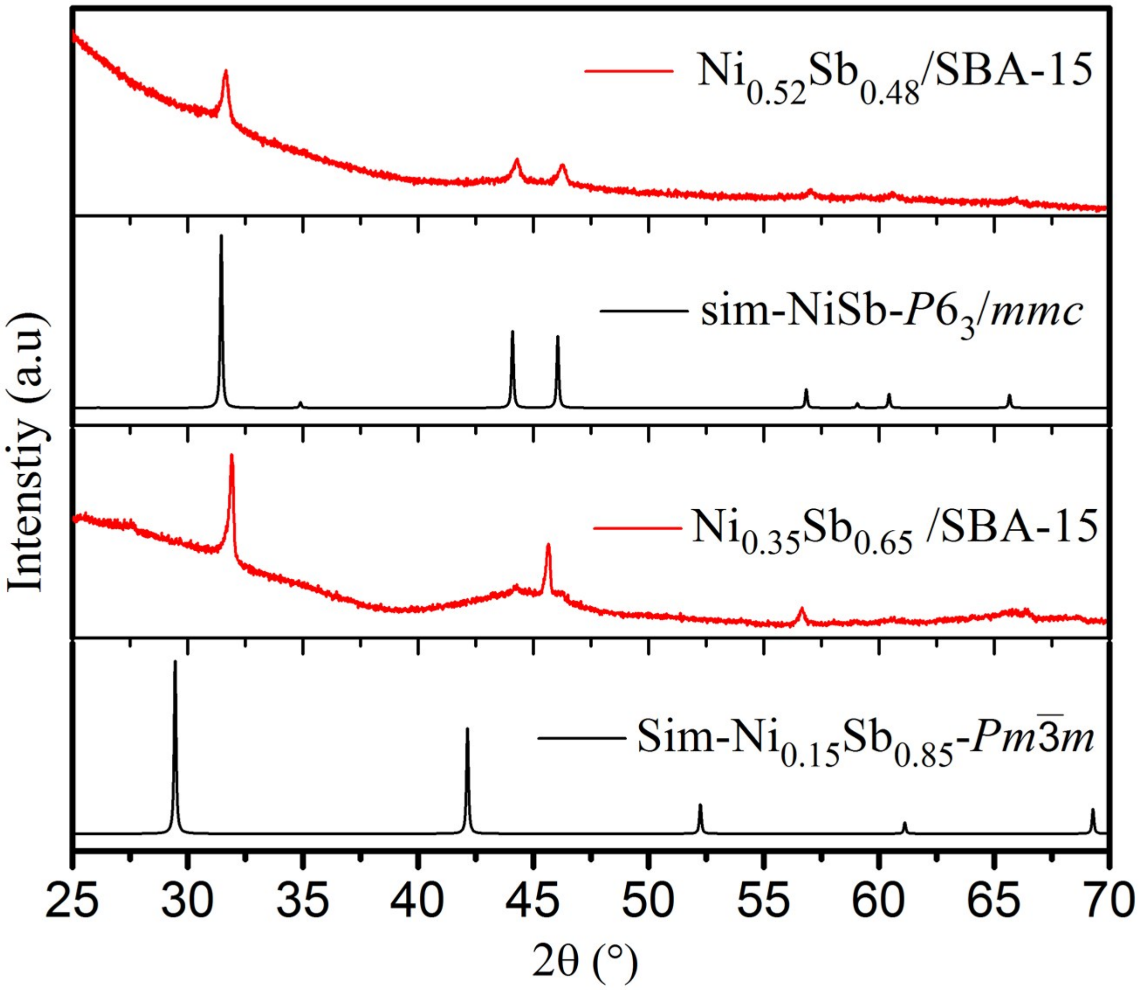

Figure S1. The comparison of PXRD pattern of $Ni_{0.3}Sb_{0.7}$/SBA-15 and $Ni_{0.52}Sb_{0.48}$/SBA-15 with $Ni_{0.15}Sb_{0.85}$ and NiSb simulated patterns.

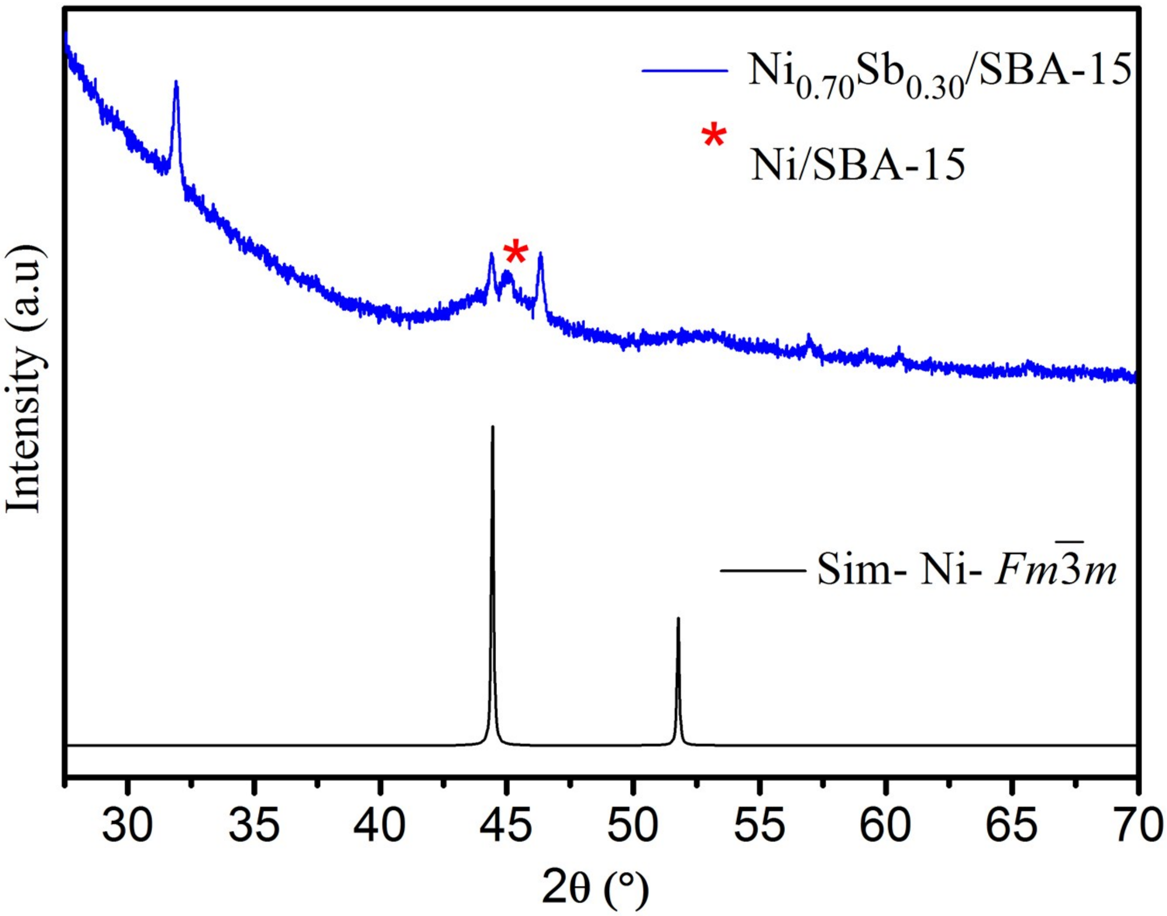

Figure S2. The comparison of PXRD of $Ni_{0.7}Sb_{0.3}$/SBA-15 with simulated Ni XRD pattern.

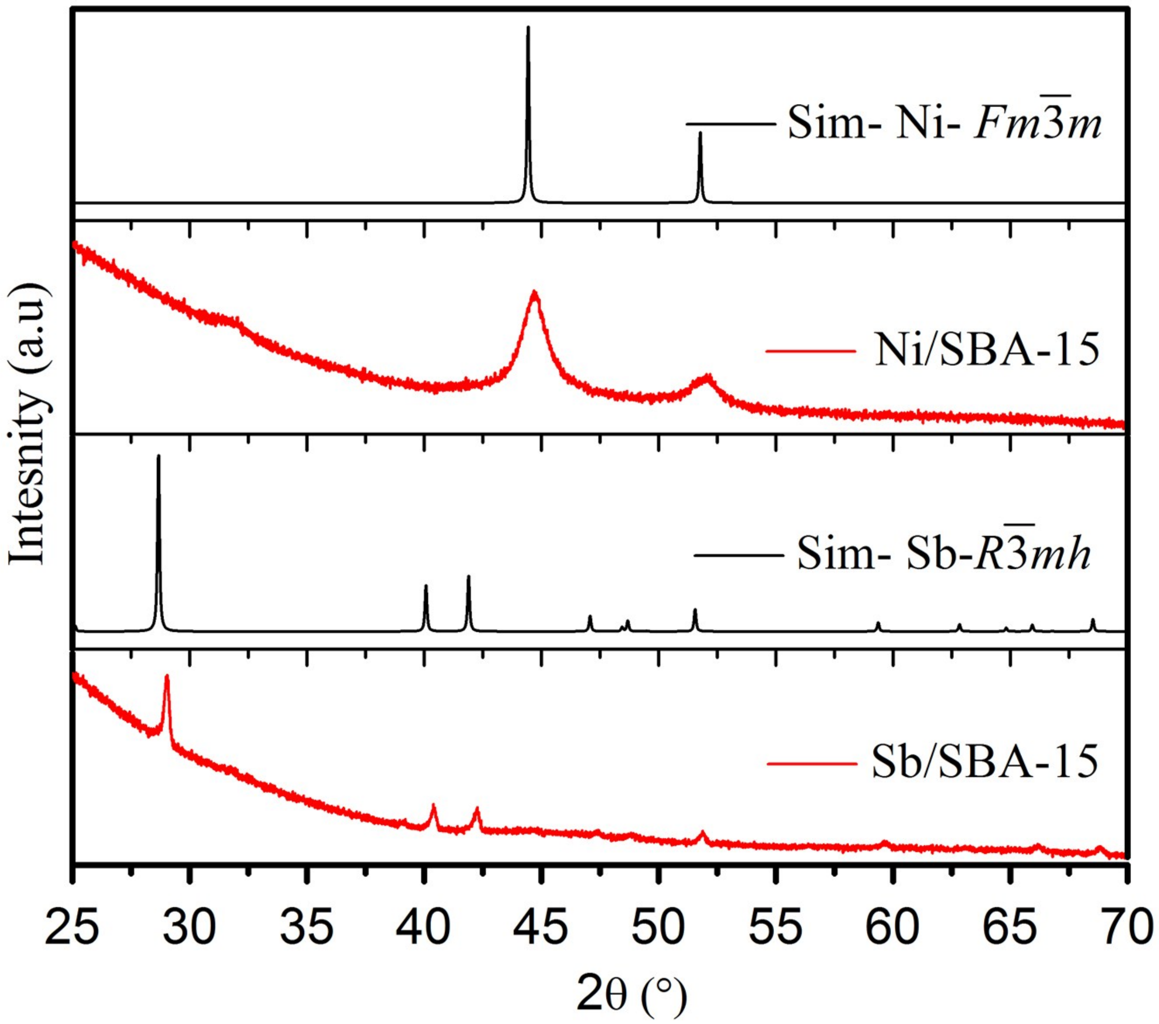

Figure S3. The comparison of XRD pattern of monometallic Ni and Sb supported SBA-15 with Ni and Sb simulated patterns.

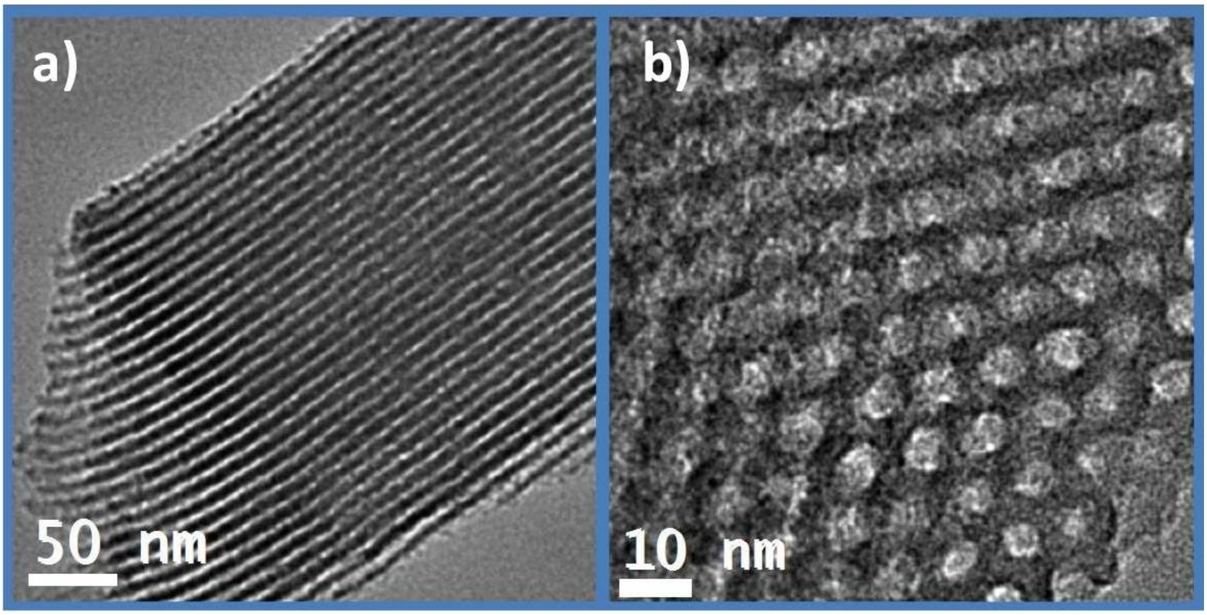

FigureS4.TEM images of SBA-15 showing a) well ordered hexagonal planes and b) Pore openings.

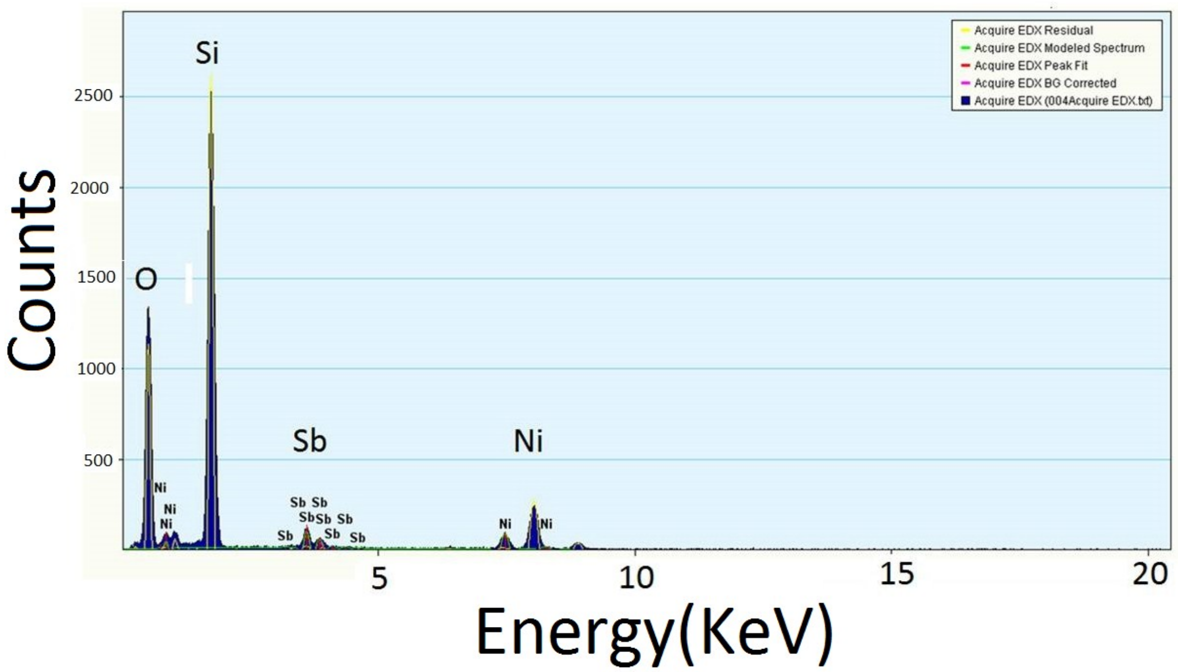

Figure S5. TEM-EDAX of $Ni_{0.52}Sb_{0.48}$/SBA-15 catalyst.

.

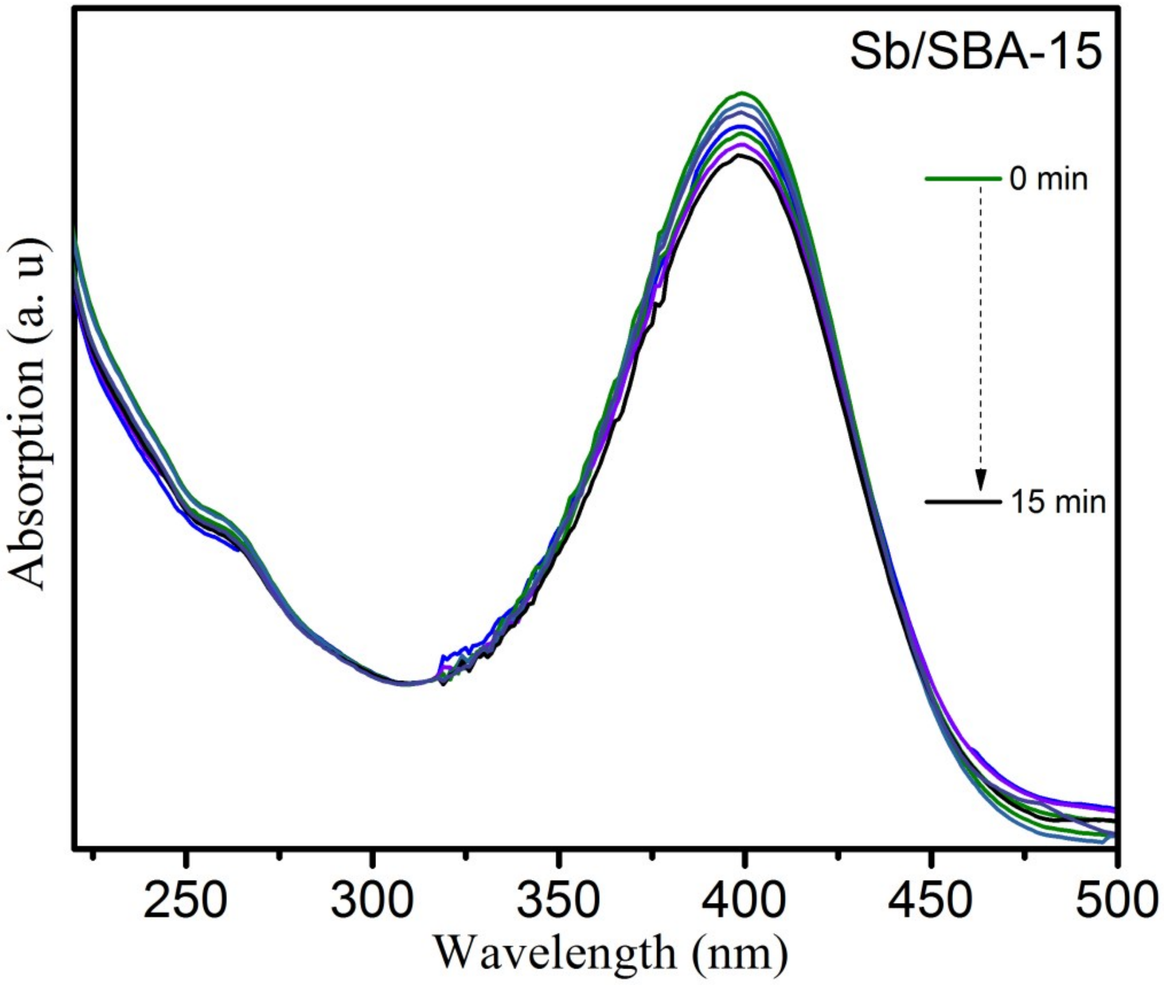

Figure S6.UV-Vis absorption spectra for the reduction of p-NP to p-AP by Sb/SBA-15 catalyst.

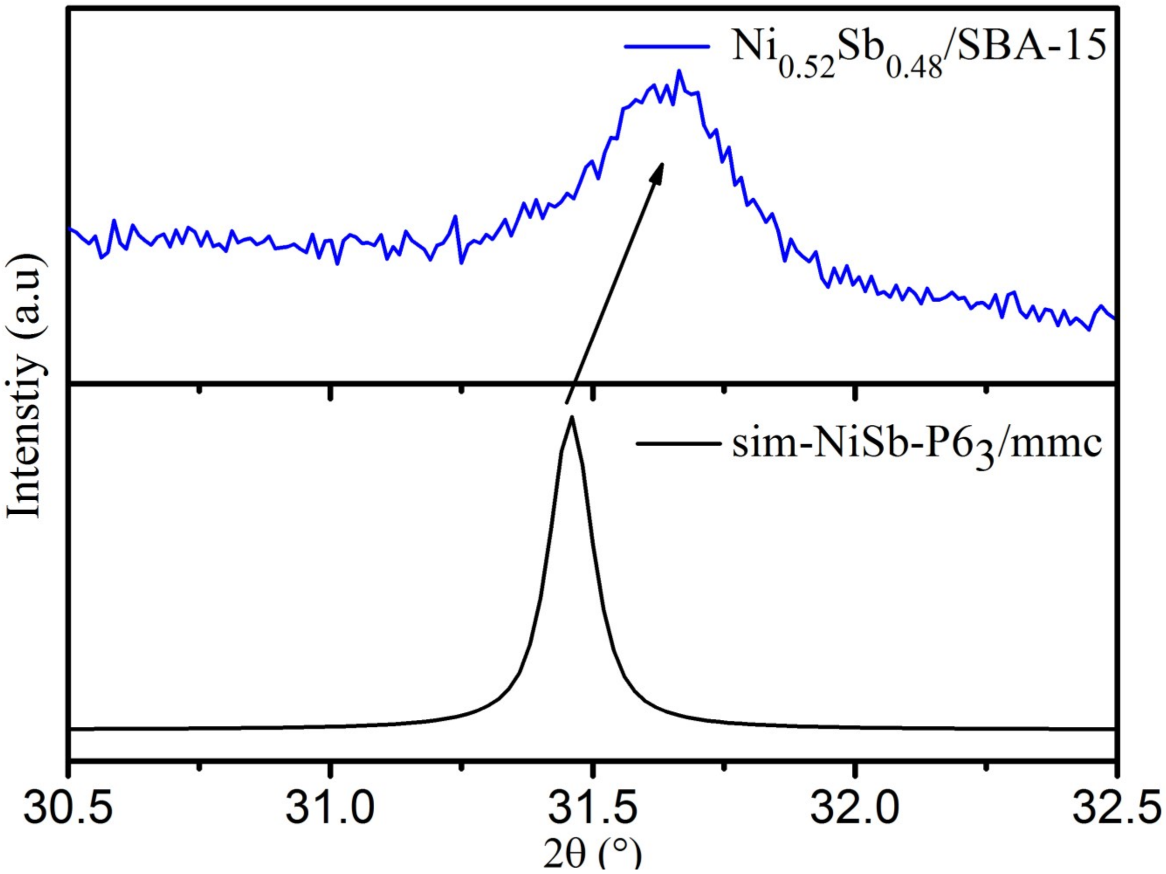

FigureS7. Powder XRD comparison of the main peak corresponding to (101) plane of NiSb/SBA-15 catalyst with the corresponding simulated bulk material.

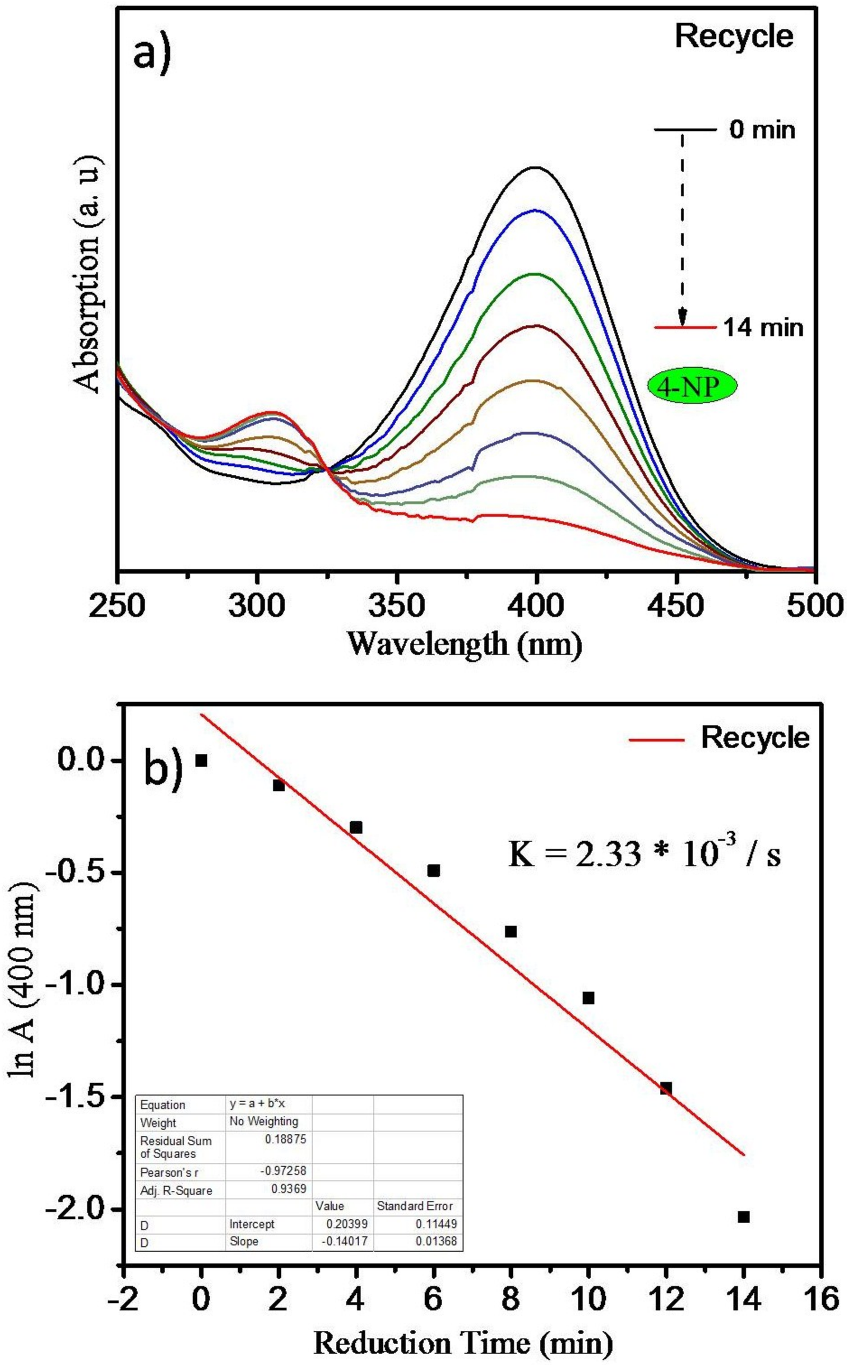

Equation	y = a + b*x		
Weight	No Weighting		
Residual Sum of Squares	0.18875		
Pearson's r	-0.97258		
Adj. R-Square	0.9369		
		Value	Standard Error
D	Intercept	0.20399	0.11449
D	Slope	-0.14017	0.01368

Figure S8.UV-Vis absorption spectra (a) and plot of ln A of 4-NA at 400 nm vs. reduction time (b) for the reduction of p-NA to PPD by$Ni_{0.52}Sb_{0.48}$/SBA-15.

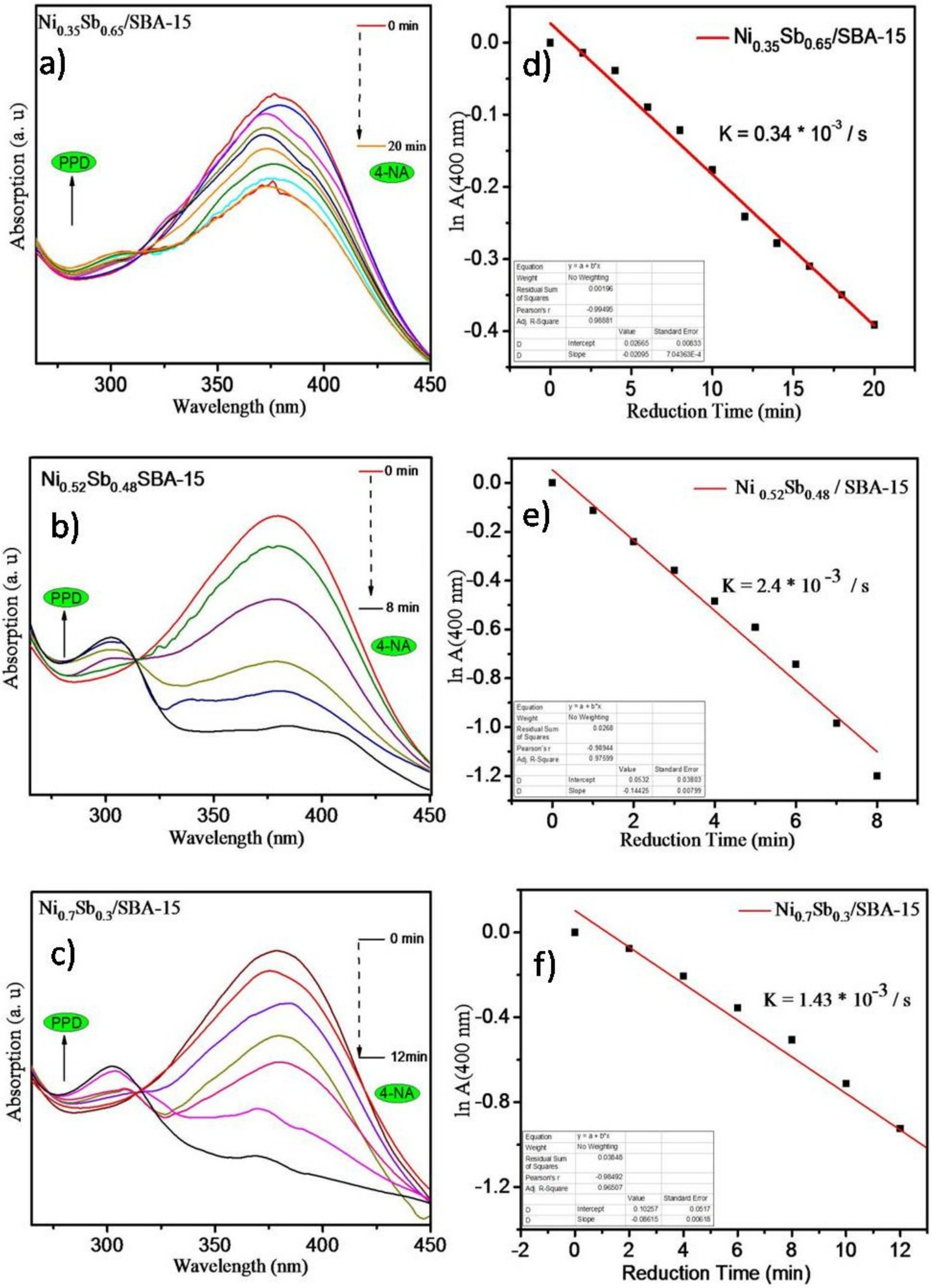

Figure S9. UV-Vis absorption spectra and plot of ln A of p-nitro aniline at 400 nm vs. reduction time for the reduction of p-nitroaniline to p-phenylenediamine by $Ni_{0.35}Sb_{0.65}$/SBA-15(and d), $Ni_{0.52}Sb_{0.48}$/SBA-15 (band e) and $Ni_{0.70}Sb_{0.30}$/SBA-15 (c and f).

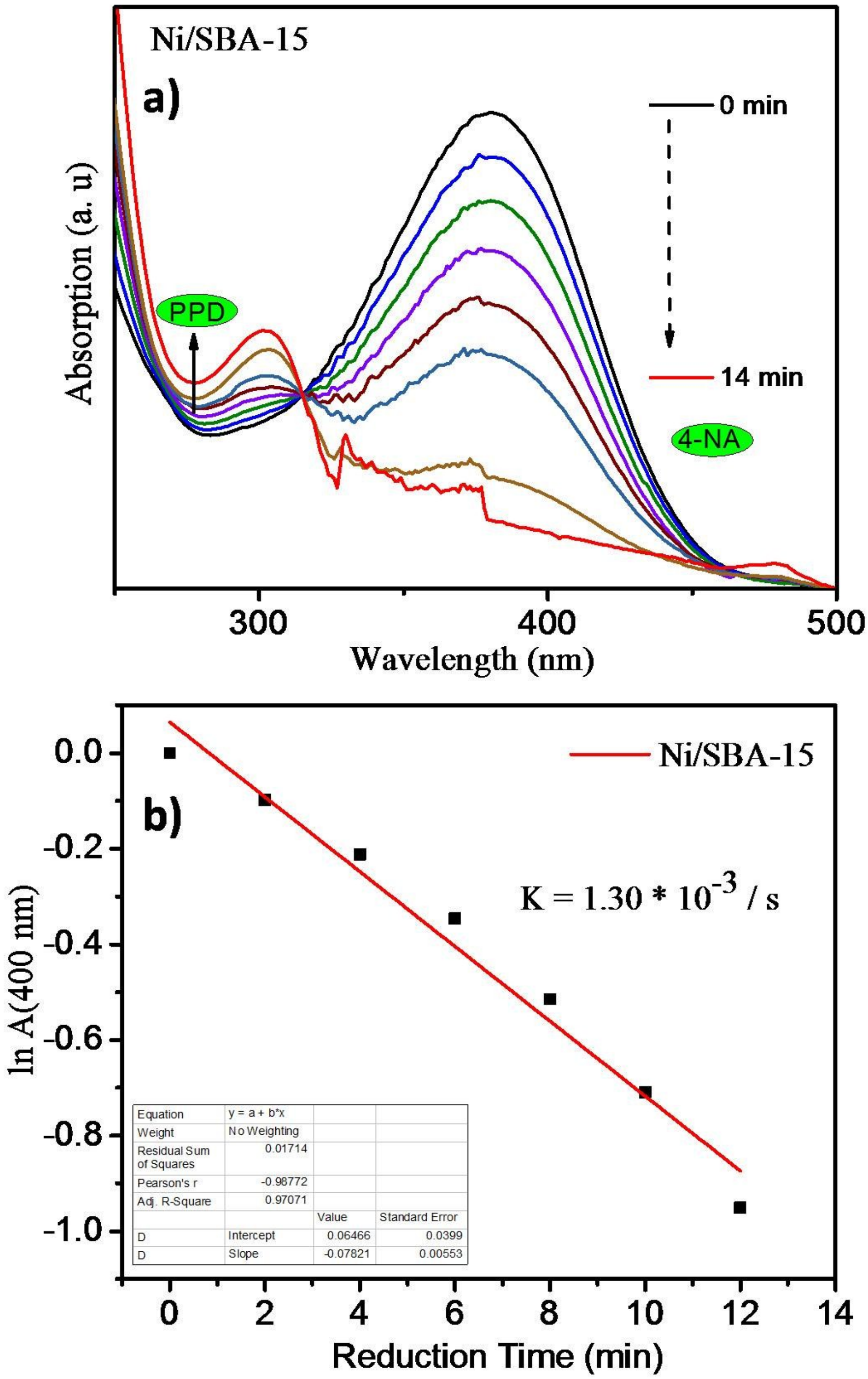

Equation	y = a + b*x		
Weight	No Weighting		
Residual Sum of Squares	0.01714		
Pearson's r	-0.98772		
Adj. R-Square	0.97071		
		Value	Standard Error
D	Intercept	0.06466	0.0399
D	Slope	-0.07821	0.00553

FigureS10. UV-Vis absorption spectra (a) and plot of ln A of p-nitro aniline at 400 nm vs. reduction time (b) for the reduction of p-nitroaniline to p-phenylenediamine by Ni /SBA-15.

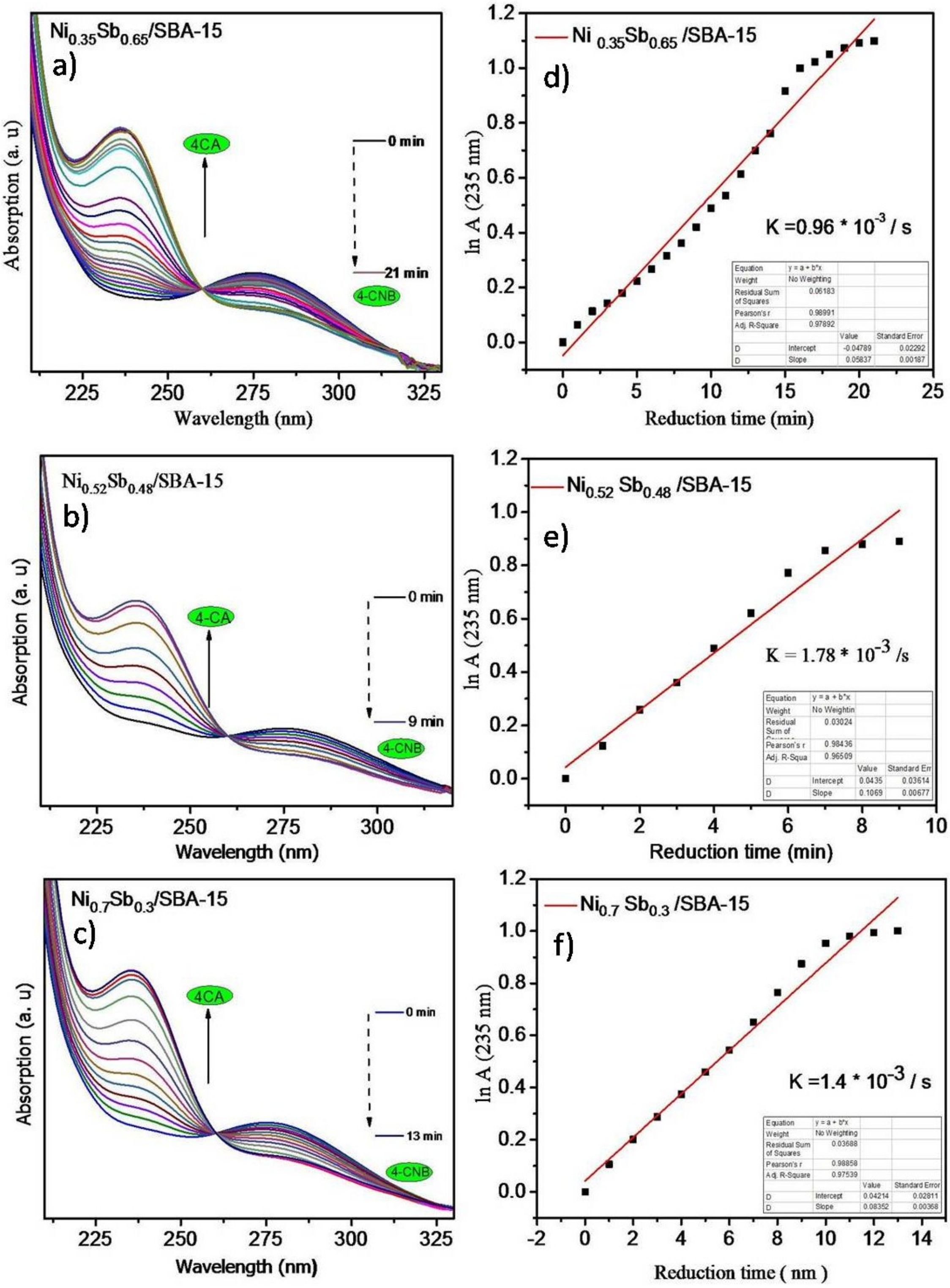

Equation	y = a + b*x		
Weight	No Weighting		
Residual Sum of Squares	0.06183		
Pearson's r	0.98991		
Adj. R-Square	0.97892		
		Value	Standard Error
D	Intercept	-0.04789	0.02292
D	Slope	0.05837	0.00187

Equation	y = a + b*x		
Weight	No Weightin		
Residual Sum of	0.03024		
Pearson's r	0.98436		
Adj. R-Squa	0.96509		
		Value	Standard Err
D	Intercept	0.0435	0.03614
D	Slope	0.1069	0.00677

Equation	y = a + b*x		
Weight	No Weighting		
Residual Sum of Squares	0.03688		
Pearson's r	0.98858		
Adj. R-Square	0.97539		
		Value	Standard Error
D	Intercept	0.04214	0.02811
D	Slope	0.08352	0.00368

FigureS11.UV-Vis absorption spectra and plot of ln A of p-chloronitrobenzene at 235 nm vs. reduction time for the reduction of p-chloronitrobenzene (4CNB) to p-chloroaniline (4CA) by Ni$_{0.35}$Sb$_{0.65}$/SBA-15(and d), Ni$_{0.52}$Sb$_{0.48}$/SBA-15 (band e) and Ni$_{0.70}$Sb$_{0.30}$/SBA-15 (c and f).

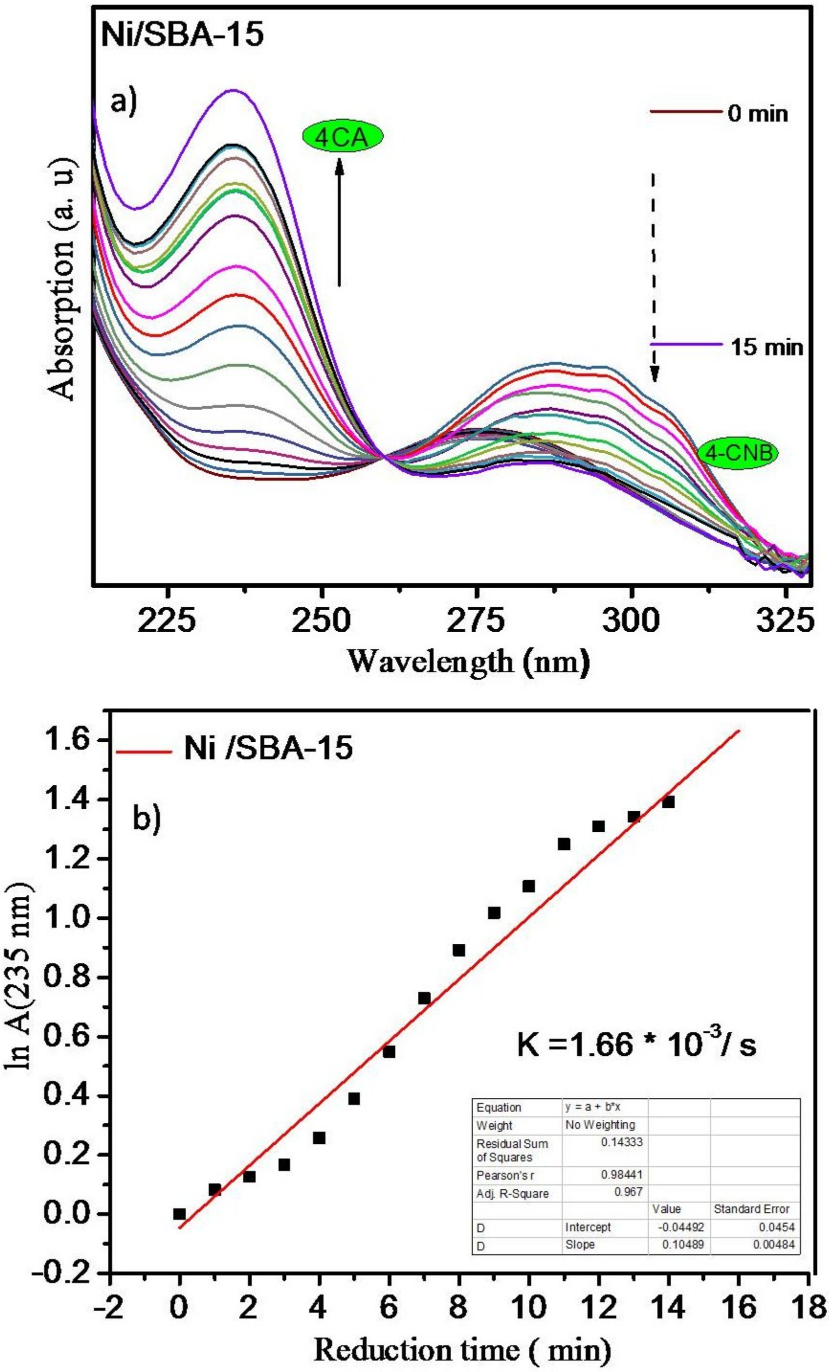

Equation	y = a + b*x		
Weight	No Weighting		
Residual Sum of Squares	0.14333		
Pearson's r	0.98441		
Adj. R-Square	0.967		
		Value	Standard Error
D	Intercept	-0.04492	0.0454
D	Slope	0.10489	0.00484

FigureS12.UV-Vis absorption spectra (a) and plot of ln A of p-chloronitrobenzene at 235 nm vs. reduction time (b) for the reduction of p-chloronitrobenzene (4-CNB) to p-chloroaniline (4CA) by Ni /SBA-15.

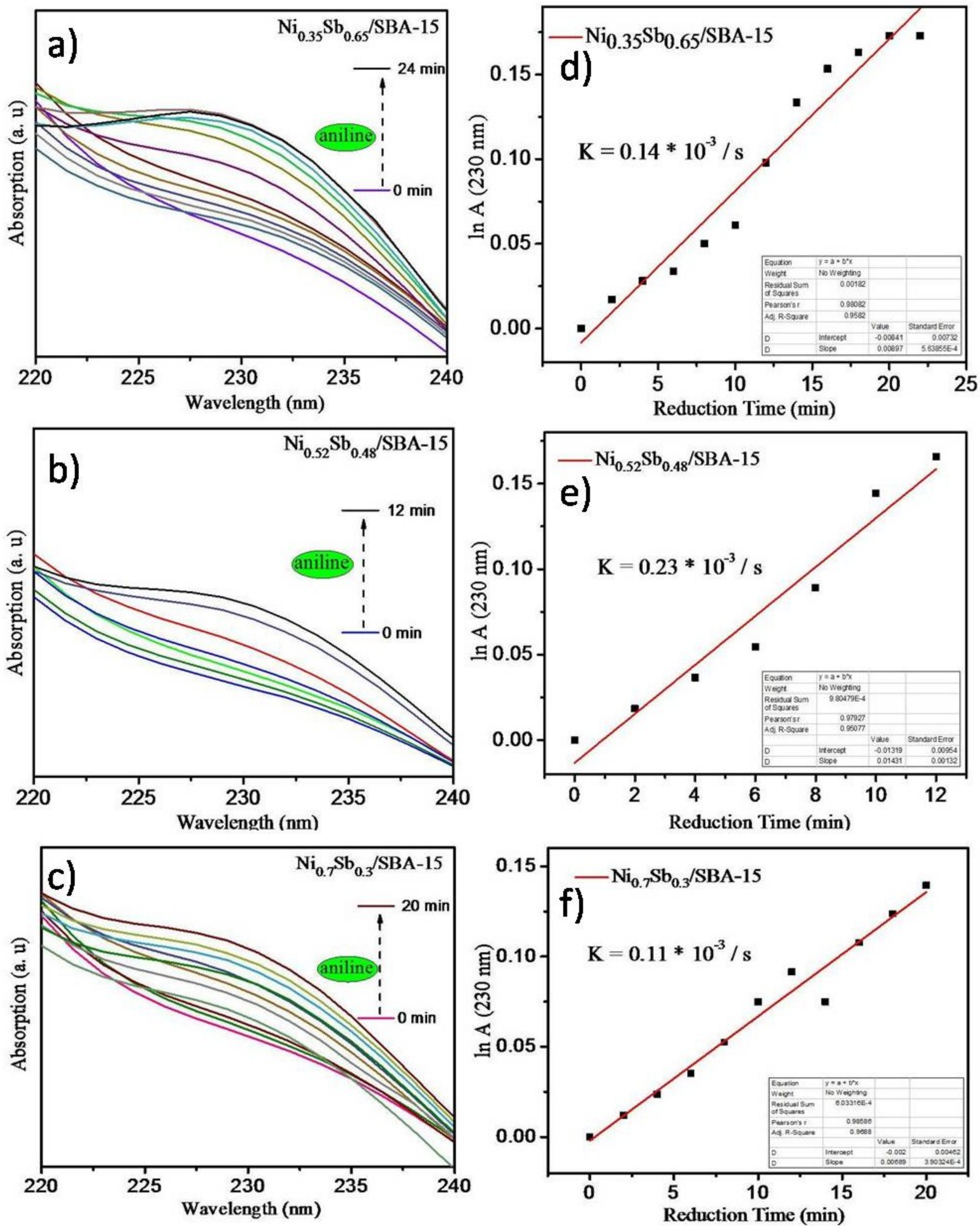

Equation	y = a + b*x		
Weight	No Weighting		
Residual Sum of Squares	0.00182		
Pearson's r	0.98082		
Adj. R-Square	0.9582		
		Value	Standard Error
D	Intercept	-0.00841	0.00732
D	Slope	0.00897	5.63855E-4

Equation	y = a + b*x		
Weight	No Weighting		
Residual Sum of Squares	9.80479E-4		
Pearson's r	0.97927		
Adj. R-Square	0.95077		
		Value	Standard Error
D	Intercept	-0.01319	0.00954
D	Slope	0.01431	0.00132

Equation	y = a + b*x		
Weight	No Weighting		
Residual Sum of Squares	6.03316E-4		
Pearson's r	0.98586		
Adj. R-Square	0.9688		
		Value	Standard Error
D	Intercept	-0.002	0.00462
D	Slope	0.00689	3.90324E-4

FigureS13. UV-Vis absorption spectraand plot of ln A of nitrobenzene at 230 nm vs. reduction time for the reduction of nitrobenzeneto aniline by $Ni_{0.35}Sb_{0.65}$/SBA-15(aand d), $Ni_{0.52}Sb_{0.48}$/SBA-15 (band e) and $Ni_{0.70}Sb_{0.30}$/SBA-15 (c and f).

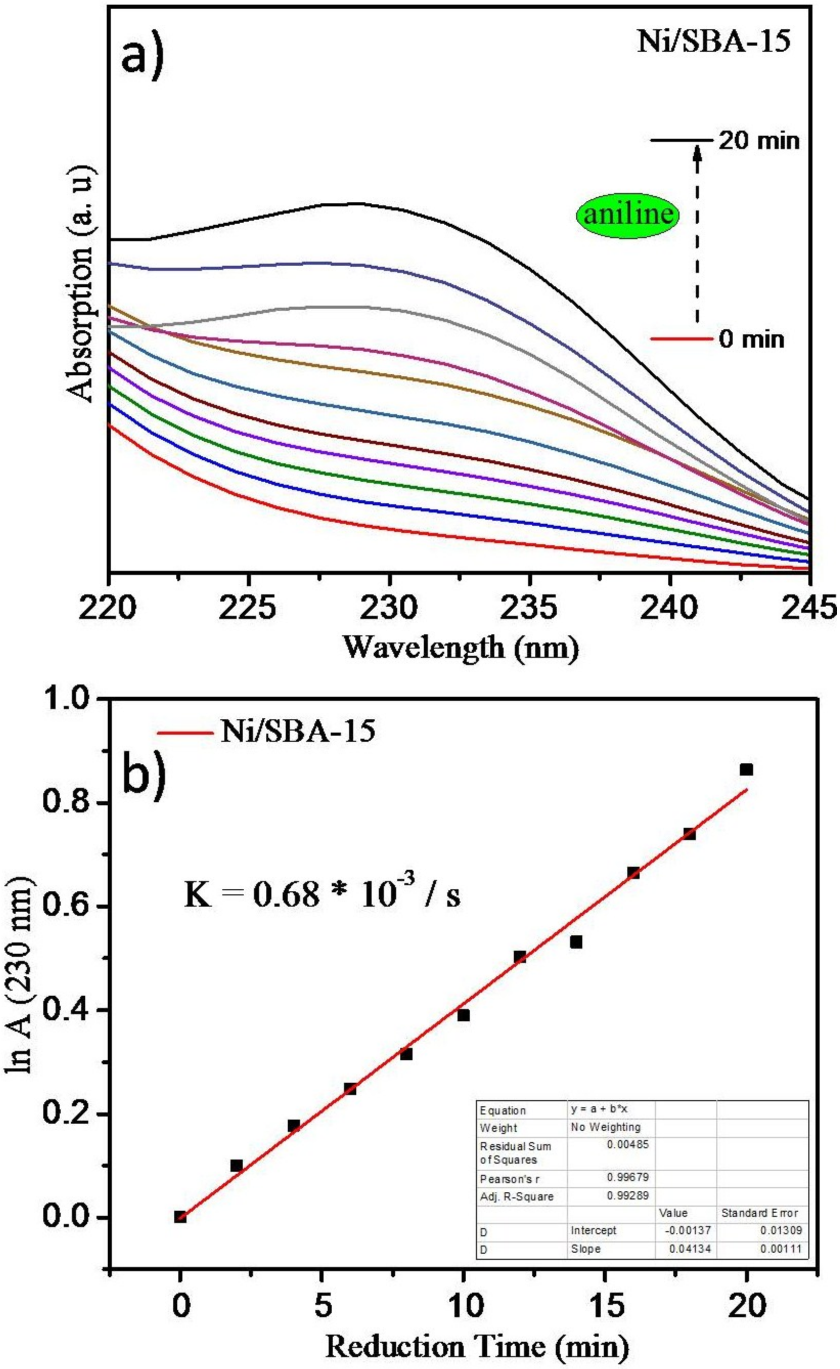

Equation	y = a + b*x		
Weight	No Weighting		
Residual Sum of Squares	0.00485		
Pearson's r	0.99679		
Adj. R-Square	0.99289		
		Value	Standard Error
D	Intercept	-0.00137	0.01309
D	Slope	0.04134	0.00111

FigureS14.UV-Vis absorption spectra (a) and plot of ln A of nitrobenzene at 230 nm vs. reduction time (b) for the reduction of nitrobenzeneto aniline byNi /SBA-15.